doi:10.4149/neo_2020_191029N1102

Long non-coding RNA CASC2 enhances cisplatin sensitivity in oral squamous cell cancer cells by the miR-31-5p/KANK1 axis

J. WANG[1], J. JIA[2], L. ZHOU[1,*]

[1]*Department of Endodontic, Qingdao Stomatological Hospital, Qingdao, Shandong, China;* [2]*Department of Stomatology, Taian City Central Hospital, Taian, Shandong, China*

**Correspondence: gipxvj@163.com*

Received October 29, 2019 / Accepted June 3, 2020

Oral squamous cell cancer (OSCC) is a primary malignant tumor of the head and neck. Long non-coding RNA cancer susceptibility candidate 2 (CASC2) is related to the chemoresistance of diverse tumors. At present, the resistance of OSCC to first-line chemotherapy drug cisplatin (DDP) is still a giant problem. Herein, we investigated the role and mechanism of CASC2 in OSCC resistance to DDP. Expression levels of CASC2, miR-31-5p, and KANK1 in OSCC tissues and cells were determined by qRT-PCR. The half-maximal inhibitory concentration (IC50) value of DDP-resistant OSCC cells and apoptosis of DDP-resistant OSCC cells were determined via CCK-8 or flow cytometry assays. The relationship between CASC2 or KANK1 and miR-31-5p was verified with a dual-luciferase reporter or RIP assays. The role of CASC2 *in vivo* was confirmed by xenograft experiments. We observed that CASC2A and KANK1 were downregulated while miR-31-5p was upregulated in DDP-resistant OSCC tissues and cells ($p<0.05$). CASC2 overexpression enhanced cell DDP sensitivity and accelerated cell apoptosis in DDP-resistant OSCC cells *in vivo* and *in vitro* ($p<0.05$). Notably, KANK1 acted as a target for miR-31-5p. Also, CASC2 modulated KANK1 expression via sponging miR-31-5p in DDP-resistant OSCC cells ($p<0.05$). Both CASC2 and KANK1 introduction-mediated impacts on the DDP sensitivity and apoptosis of DDP-resistant OSCC cells were restored by miR-31-5p elevation ($p<0.05$). To conclude, CASC2 boosted the DDP sensitivity and apoptosis of DDP-resistant OSCC cells by upregulating KANK1 via sponging miR-31-5p, and CASC2 might be a potential target for DDP-resistant OSCC treatment.

Key words: oral squamous cell cancer (OSCC), CASC2, miR-31-5p, KANK1, DDP, resistance

Oral squamous cell cancer (OSCC) is a major malignancy of the head and neck with high local infiltration and cervical lymph node metastasis [1]. Currently, radical surgery combined with adjuvant chemotherapy remains the most effective method for the treatment of OSCC [2]. However, the overall 5-year survival rate for OSCC patients is still less than 50% [3]. Also, the main cause of distant metastasis and local recurrence of OSCC are related to anti-cancer resistance [4], clinical TNM stage [5], and the size of surgical margins [6]. Cisplatin (DDP) is commonly used as a first-line chemotherapy regimen for the treatment of OSCC, but it usually fails due to the rapid development of chemoresistance [7]. Hence, it is vital to understand the molecular mechanism of DDP resistance in OSCC for improving the prognosis of patients with OSCC.

Long non-coding RNAs (lncRNAs) are a category of outstanding non-protein-encoding RNAs that exert vital regulatory roles in gene regulatory networks, such as their involvement in physiological and pathological processes, including organogenesis and tumorigenesis [8, 9]. Studies have revealed that the chemoresistance of a range of tumors was connected with abnormal expression of lncRNA, including OSCC [10, 11]. Long non-coding RNA cancer susceptibility candidate 2 (CASC2), located on chromosome 10q26, was first discovered to be reduced in endometrial cancer [12]. Also, CASC2 was pointed out to be associated with the chemoresistance of multiplex tumors, such as glioma [13], hepatocellular cancer [14], cervical cancer [15], and other malignancies. Besides, downregulated CASC2 expression was disclosed to promote the progression of OSCC [16]. However, the role and mechanism of CASC2 in OSCC-resistant DDP have not been reported.

microRNAs (miRNAs) are another kind of non-coding RNAs that play their function primarily by suppressing mRNA translation or causing mRNA degradation [17]. They are involved in a series of biological processes, including

cell proliferation, differentiation, migration, and apoptosis [18]. microRNA-31-5p (miR-31-5p) has been reported as a carcinogen or suppressor in different tumors [19, 20]. Furthermore, miR-31-5p could accelerate sorafenib and oxaliplatin resistance in renal cell cancer [21] or hepatocellular cancer [22]. Moreover, miR-31-5p could elevate the tumorigenicity of OSCC [23]. Previous research reported that miR-31 might be a downstream target of CASC2 [24]. However, the relationship between miR-31-5p and CASC2 has not been confirmed so far.

KN motif and ankyrin repeat domain-containing protein 1 (KANK1) is a member of the KANK family [25], which can mediate the construction of the cytoskeleton by effecting the polymerization of actin [26]. Also, KANK1 depletion promoted the centrosomal amplification [27]. Moreover, it was proved as a suppressor in various tumors [28–30]. For instance, KANK1 impeded the progression of human malignant peripheral nerve sheath tumors via promoting cell apoptosis [29]. Nevertheless, the role of KANK1 in DDP resistance in OSCC is unclear.

Consequently, we aimed to explore the role and molecular mechanism of CASC2 in the chemoresistance of OSCC to DDP and provide possible targets for enhancing the chemosensitivity and prognosis of OSCC patients.

Patients and methods

Patients OSCC specimen's collection. This study was approved by the Ethics Committee of the Qingdao Stomatological Hospital. Twenty-five paired specimens used in this study were obtained from patients with OSCC who were diagnosed via pathological detection based on the World Health Organization histologic grading system [30] and treated at Qingdao Stomatological Hospital. The sample selection criteria were: patients over 18 years of age, tumors located in the mouth (from the lips to the beginning of the oropharynx), and no other cancer diseases, and TNM stage meeting the revised American Joint Committee on Cancer (AJCC) criteria [31, 32]. Also, all participants in this study signed informed consent. According to National Comprehensive Cancer Network (NCCN) treatment guidelines for DDP treatment of OSCC patients, based on the chemotherapy response, 12 patients with tumor shrinkage were divided into sensitive groups, and 13 patients with tumor volume development or stability were divided into drug-resistant groups. The clinical characteristics of OSCC patients are shown in Table 1.

Table 1. Correlation between CASC2 expression and clinical characteristics of OSCC patients.

Characteristics	Total number	High expression (n=12)	Low expression (n=13)	p-value
Age				0.2377
<60	11	7	4	
≥60	14	5	9	
Gender				0.6951
Male	12	5	7	
Female	13	7	6	
Smoking history				0.4283
Yes	15	6	9	
No	10	6	4	
Lymph node metastasis				0.0302*
Yes	7	6	1	
No	18	6	12	
TNM stage				0.0414*
I–II	9	7	2	
III–IV	16	5	11	

High or Low CASC2 expression was obtained by the sample mean. The relation between CASC2 expression and clinicopathological characteristics was determined via Pearson χ^2 test. *p<0.05 was deemed statistically significant

Cell culture and treatment. Human normal oral keratinocyte cell line NOK-SI was acquired from Mingzhou Biotechnology Co., Ltd. (Hangzhou, China). 293T and OSCC cells (CAL-27 and SCC9) were purchased from the American Type Culture Collection (Rockville, MD, USA). Dulbecco's Modified Eagle Medium (DMEM, Invitrogen, Carlsbad, CA, USA) was used to culture NOK-SI, CAL-27, and SCC9 cells. Eagle's Minimum Essential Medium (EMEM) from Sigma-Aldrich (St. Louis, MO, USA) was utilized for the maintenance of the 293T cells. DDP (Sigma-Aldrich)-resistant OSCC cells were obtained from parental CAL-27 and SCC9 cells by gradually elevating the doses of DDP in DMEM for about 6–8 months [33]. CAL-27/DDP and SCC9/DDP cells were cultured in DMEM with DDP (5 μM) for 48 h for passage.

Cell transfection. The sequences of CASC2 and KANK1 were synthesized and cloned into the pcDNA3.1 vector (Vector) (Thermo Fisher Scientific, Waltham, MA, USA) to obtain the overexpression vectors of CASC2 (Over-CASC2) and KANK1 (Over-KANK1). miRNA mimic targeting miR-31-5p (miR-31-5p mimic) and negative control (miR-NC) were purchased from GenePharma (Shanghai, China). Oligonucleotides or vectors were transfected into CAL-27/DDP and SCC9/DDP cells using Lipofectamine 3000 reagents (Invitrogen) [34]. The sequence of miR-31-5p mimic was displayed as the following: miR-31-5p mimic (5'-AGGCAAGAUGCUGGCAUAGCU-3').

Quantitative real-time polymerase chain reaction (qRT-PCR). TRIzol reagent (Invitrogen) was applied to extract the total RNA. Total RNA was reverse transcribed to complementary DNA using the PrimeScript RT reagent Kit (Takara, Dalian, China) or miRNA First-Strand Synthesis Kit (Takara). The SYBR Premix Ex Taq (Takara) was employed to carry out the qRT-PCR. The expression of CASC2, KANK1, and miR-31-5p was calculated by the $2^{-\Delta\Delta Ct}$ method and Glyceraldehyde-3-phosphate dehydrogenase (GAPDH) or U6 small nuclear RNA (snRNA) served as an internal control [35]. The primers were exhib-

ited as below: CASC2: (F: 5'-GCACATTGGACGGTGTTTCC-3' and R: 5'-CCCAGTCCTTCACAGGTCAC-3'); miR-31-5p: (F: 5'-TATTCATAGGCAAGATGCTGGC-3' and R: 5'-TATGGTTGTTCTCGTCTCCTTCTC-3'); KANK1 (F: 5'-GCAAGAAGAGAAAAGGCAGTTG-3' and R: 5'-TCCTCACACCACAGACATTGAT-3'); GAPDH: (F: 5'-GACTCCACTCACGGCAAATTCA-3' and R: 5'-TCGCTCCTGGAAGATGGTGAT-3'); U6 snRNA (F: 5'-GCTCGCTTCGGCAGCACA-3', R: 5'-GAGGTATTCGCACCAGAGGA-3').

Cell viability assay. According to previous descriptions, the viability of CAL-27/DDP and SCC9/DDP cells was detected through the Cell Counting Kit-8 (CCK-8, Dojindo, Gaithersburg, MD, USA) [36]. CAL-27/DDP and SCC9/DDP cells (3×10^3 cells/well) were cultured in different doses of DDP for 48 h. Then, the CCK-8 solution was replenished to each well and maintained for 2 h. Subsequently, the Microplate Reader (Thermo Fisher Scientific) was used to assess the optical density (OD) at 450 nm.

Flow cytometry assay. Apoptosis detection was performed according to the previous description [37]. Annexin V-fluorescein isothiocyanate (FITC)/propidium iodide (PI) apoptosis detection kit (BD Biosciences, San Jose, CA, USA) was used to detect the apoptosis rate of cells was. Briefly, CAL-27/DDP and SCC9/DDP cells were harvested and resuspended in binding buffer (1×10^5 cells/ml). Afterward, Annexin V-FITC (10 μl) and PI (5 μl) were complemented to the above binding buffer and incubated for 15 min. Eventually, the FACScan flow cytometry (BD Biosciences) was employed to analyze the apoptosis rate of CAL-27/DDP and SCC9/DDP cells.

Western blot analysis. Radio-immunoprecipitation assay (RIPA) lysis buffer (Invitrogen) was applied to extract total protein. A previous study was referenced to perform western blot analysis [38]. The primary antibodies including rabbit anti-B cell lymphoma 2 (Bcl-2, ab32124, 1:1000), rabbit anti-Bcl 2 associated X (Bax, ab32503, 1:1000), mouse anti-multidrug resistance-associated protein-1 (MRP-1, ab32574, 1:500) and mouse anti-GAPDH (ab8245, 1:500). Next, the PVDF membrane was incubated with goat anti-rabbit (ab97051, 1:2000) or anti-mouse immunoglobulin G (IgG, ab205719, 1:2000). Finally, the Immobilon™ Western Chemiluminescent HRP Substrate (Millipore) was applied to visualize the protein bands. All antibodies used in this study were purchased from Abcam (Cambridge, MA, USA) and GAPDH was deemed as a loading control.

Dual-luciferase reporter assay. The miRcode tool or starBase 2.0 was employed for the prediction of the possible binding sites between CASC2 or KANK1 and miR-31-5p. Dual-luciferase reporter assay was based on a previous study [39]. In short, the sequences of wild type CASC2 (with predicted miR-31-5p binding sites), mutant CASC2, wild type KANK1 3' Untranslated Regions (UTR) (harbored potential binding sites for miR-31-5p) and mutant KANK1 3' UTR were synthesized and inserted into the pGL3-control vector (Promega, Madison, WI, USA) to construct the luciferase reporter vectors CASC2-WT, CASC2-MUT, KANK1 3' UTR-WT, and KANK1 3' UTR-MUT. Then, the miR-NC or miR-31-5p mimic was co-transfected into 293T cells with luciferase reporter vectors. Finally, the luciferase activities of luciferase reporter vectors were tested through the dual-luciferase reporter assay kit (Promega).

RNA immunoprecipitation (RIP) assay. The interaction between CASC2 and miR-31-5p was analyzed with the Magna RIP kit (Millipore). RIP assay followed a previous study [40]. In short, CAL-27/DDP and SCC9/DDP cells were lysed in RIP lysis buffer. Afterward, the lysates of CAL-27/DDP and SCC9/DDP cells were incubated in the RIP buffer possessing magnetic beads conjugated with anti-IgG or anti-Ago2 antibody (Millipore). After washing, the magnetic beads were incubated with proteinase K (Sigma-Aldrich). Subsequently, total RNA was isolated and the relative enrichment of CASC2 and miR-31-5p was analyzed by qPCR.

Tumor xenograft experiments. The animal experiments were approved by the Ethics Committee of Qingdao Stomatological Hospital. Tumor xenograft experiments refer to previous studies [41]. 24 BALB/c nude mice (five-week-old) were obtained from the Shanghai Experimental Animal Center (Shanghai, China). SCC9/DDP cells were transfected with Vector or lentivirus-mediated Over-CASC2. Then, SCC9/DDP cells (1×10^6 cells) were subcutaneously injected into the dorsal side of each nude mouse. After tumor formation, mice were injected intraperitoneally with DDP (0.4 mg/kg) or an equivalent amount of PBS three times a week. The tumor volume of nude mice was measured every 4 days from day 7. A digital caliper was used to measure the tumor volume. The tumor volume was calculated with the equation: Volume = (length × width^2)/2. After 31 days, the mice were euthanized under anesthesia to take their tumor tissue and weighted. After weighing, all tumor tissues were frozen for subsequent study.

Statistical analysis. The data for this study were derived from 3 independent experiments and exhibited as mean ± standard deviation. SPSS 18.0 software (SPSS, Chicago, IL, USA) and GraphPad Prism 6.0 (GraphPad, San Diego, CA, USA) were utilized for statistical analysis. The normality of the distribution data in each group was determined by the Kolmogorov-Smirnov test. The differences between the two groups were assessed with Student's t test. One-way variance analysis (ANOVA) followed by Tukey post-hoc test was used to compare the differences among three or more groups. A p-value <0.05 was considered statistically significant. The relation between CASC2 expression and clinicopathological characteristics was determined via the Pearson χ^2 test. The correlation between CASC2 and miR-31-5p as well as between KANK1 and miR-31-5p in OSCC tissues were assessed via Spearman's correlation analysis.

Results

Expression of CASC2 in DDP-resistant OSCC tissues and cells. At the outset, we assessed the expression pattern of CASC2 in 25 paired OSCC tissues and adjacent healthy tissues by qRT-PCR. Compared to the adjacent healthy tissues, CASC2 expression was conspicuously reduced in OSCC tissues (Figure 1A). And high CASC2 expression was correlated with lymph node metastasis and TNM stage in OSCC patients (Table 1). Moreover, the expression of CASC2 was exceptionally lower in DDP-resistant OSCC tissues than that in DDP-sensitive OSCC tissues (Figure 1B). Additionally, CASC2 was specially downregulated in normal (CAL-27 and SCC9) and resistant (CAL-27/DDP and SCC9/DDP) OSCC cells compared with the NOK-SI cells, and CASC2 expression was apparently lower in resistant OSCC cells versus normal OSCC cells (Figures 1C, 1D). Together, these results suggested that low CASC2 expression might be related to the resistance of OSCC cells to DDP.

CASC2 upregulation elevated DDP sensitivity and cell apoptosis in DDP-resistant OSCC cells. In consideration of the above findings, we further probed the role of CASC2 in DDP resistance in OSCC via gain-of-function experiments. In the first place, we determined the viability of normal and resistant OSCC cells through the CCK-8 assay. The results displayed that the viability of CAL-27 and SCC9 cells was restrained in the medium with different concentrations of DDP relative to the CAL-27/DDP and SCC9/DDP cells (Figure 2A). Moreover, the half-maximal inhibitory concentration (IC50) value of CAL-27/DDP and SCC9/DDP cells was markedly enhanced in contrast to the CAL-27 and SCC9 cells (Figure 2B). Afterward, the expression of CASC2 in CAL-27/DDP and SCC9/DDP cells transfected with Over-CASC2 or Vector was measured via qRT-PCR. The results manifested that an apparent enhancement of CASC2 was observed in CAL-27/DDP and SCC9/DDP cells transfected with Over-CASC2 compared with the Vector group, implying that the Over-CASC2 could be used for subsequent studies (Figure 2C). Also, the effects of CASC2 introduction on DDP sensitivity and cell apoptosis in CAL-27/DDP and SCC9/DDP cells were determined by CCK-8 or flow cytometry assay, respectively. CCK-8 assay indicated that CASC2 enhancement dramatically repressed the viability of CAL-27/DDP and SCC9/DDP cells in medium with

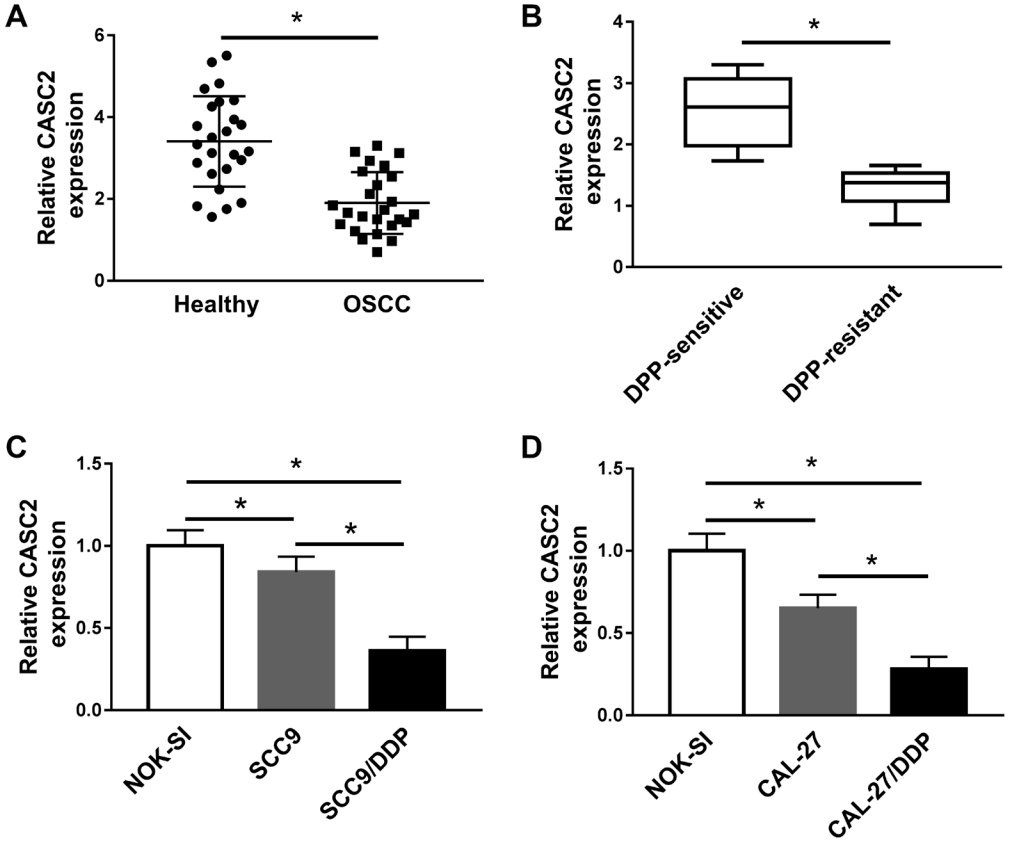

Figure 1. Expression of CASC2 was downregulated in DDP-resistant OSCC tissues and cells. A, B) The expression of CASC2 in 25 paired OSCC tissues and adjacent healthy tissues (A), as well as 13 DDP-resistant OSCC tissues and 12 DDP-sensitive OSCC tissues (B), was detected by qRT-PCR. Statistical significance was evaluated by using Student's t test. C, D) The expression of CASC2 in NOK-SI, CAL-27, SCC9, CAL-27/DDP, and SCC9/DDP cells was assessed via qRT-PCR. Statistical significance was analyzed by ANOVA followed by Tukey post-hoc test. Data were exhibited as mean ± standard deviation. *p<0.05

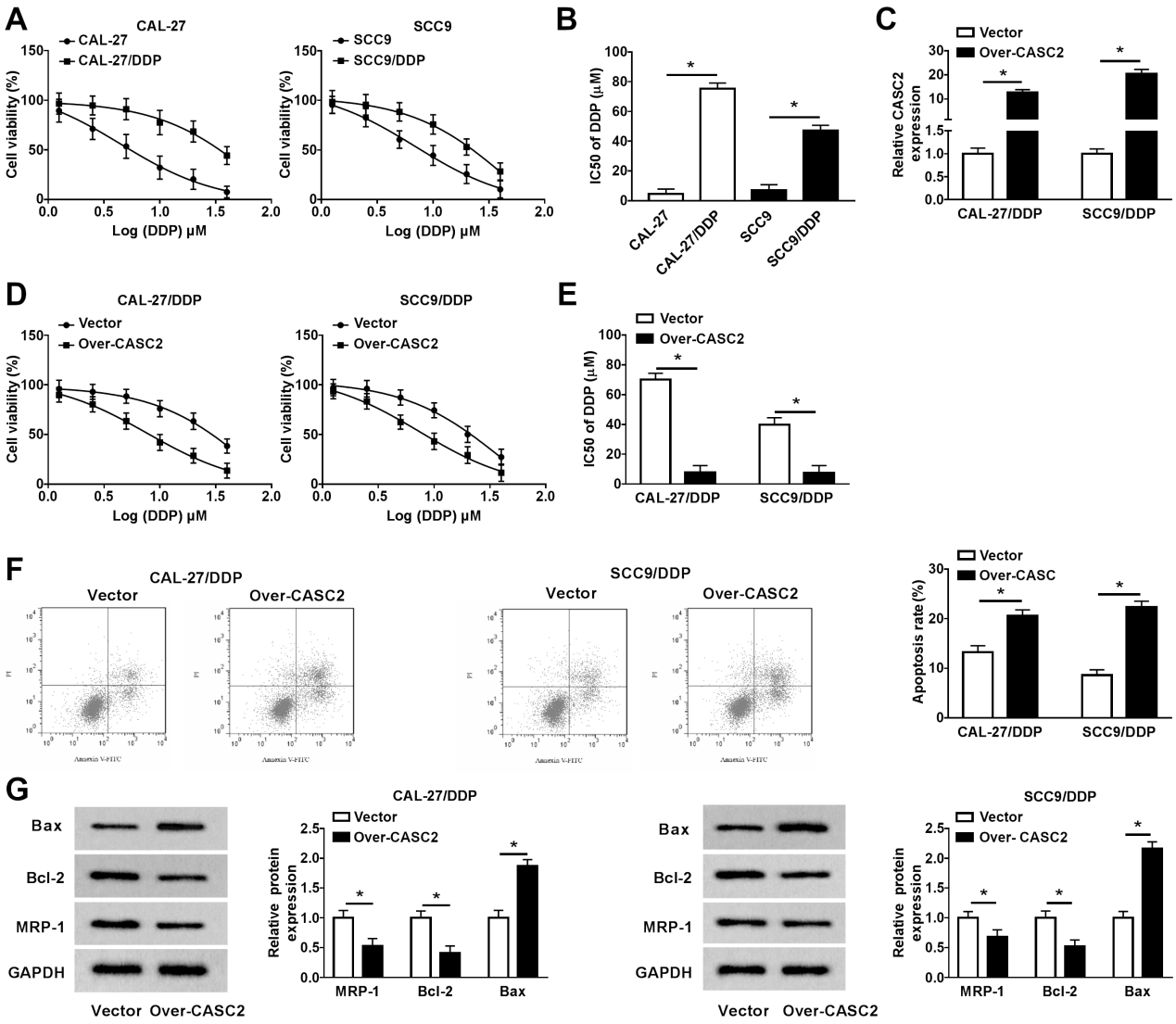

Figure 2. Effects of CASC2 overexpression on the chemosensitivity of DDP-resistant OSCC cells to DDP. A, B) The viability (A) and IC50 value (B) of CAL-27, SCC9, CAL-27/DDP, and SCC9/DDP cells were analyzed by the CCK-8 assay. C–G) CAL-27/DDP and SCC9/DDP cells were transfected with Over-CASC2 or Vector. (C) qRT-PCR was employed to assess the expression of CASC2 in CAL-27/DDP and SCC9/DDP cells. (D–E) The CCK-8 assay was executed to determine the viability (D) and IC50 value (E) of CAL-27/DDP and SCC9/DDP cells. (F) Flow cytometry assay was performed to analyze the apoptosis of CAL-27/DDP and SCC9/DDP cells. (G) Western blot analysis was applied to detect the protein levels of Bax, Bcl-2, and MRP-1 in CAL-27/DDP and SCC9/DDP cells. Statistical significance was evaluated by using Student's *t* test. Data were exhibited as mean ± standard deviation. *p<0.05

different concentrations of DDP (Figure 2D). Furthermore, the IC50 value of CASC2-elevated CAL-27/DDP and SCC9/DDP cells was distinctly reduced when compared with the control group, indicating CASC2 overexpression increased the chemosensitivity of CAL-27/DDP and SCC9/DDP cells to DDP (Figure 2E). Flow cytometry assay was then performed and the results exhibited that augmented CASC2 expression evidently facilitated the apoptosis of CAL-27/DDP and SCC9/DDP cells compared to the Vector group (Figure 2F). Besides, the protein levels of Bax, Bcl-2, and MRP-1 in CASC2-elevated CAL-27/DDP and SCC9/DDP cells were detected to verify the role of CASC2 on DDP sensitivity and cell apoptosis in resistant OSCC cells. Western blot analysis showed that overexpression of CASC2 prominently reinforced the protein level of Bax and decreased the protein levels of Bcl-2 and MRP-1 in CAL-27/DDP and SCC9/DDP cells (Figure 2G). In sum, these data suggested that augmented CASC2 expression elevated the chemosensitivity of DDP-resistant OSCC cells to DDP and promoted cell apoptosis in DDP-resistant OSCC cells.

miR-31-5p was identified to act as a target of CASC2. Next, we explored the molecular mechanisms of CASC2

in DDP resistance in OSCC to understand how CASC2 performed its function. At the outset, the expression of miR-31-5p in 25 paired OSCC tissues and adjacent healthy tissues was plumbed using qRT-PCR. The results displayed that miR-31-5p was prominently upregulated in OSCC tissues than that in adjacent healthy tissues (Figure 3A). Moreover, we found that the expression of miR-31-5p was strikingly reinforced in DDP-resistant OSCC tissues in comparison with the DDP-sensitive OSCC tissues (Figure 3B). Consistently, the expression of miR-31-5p was distinctly accelerated in CAL-27, SCC9, CAL-27/DDP, and SCC9/DDP cells than the NOK-SI cells, and miR-31-5p was dramatically higher in CAL-27/DDP and SCC9/DDP cells versus the CAL-27 and SCC9 cells (Figures 3C, 3D). Furthermore, the Spearman's correlation analysis indicated that the expression of miR-31-5p and CASC2 was negatively correlated in OSCC tissues (Figure 3E). Afterward, we discovered that miR-31-5p held the binding sites for CASC2 through miRcode tool (Figure 3F). Then, the results of the dual-luciferase reporter assay presented that miR-31-5p mimic dramatically reduced the luciferase activity of CASC2-WT in 293T cells compared with the miR-NC group, whereas the activity of CASC2-MUT was unchanged (Figure 3F). Following this, the RIP assay was employed to confirm the relationship between miR-31-5p and CASC2. We found that miR-31-5p and CASC2 were abundantly reinforced in Ago2-containing beads when compared with those with control IgG antibody in CAL-27/DDP and SCC9/DDP cells (Figure 3G). In short, these findings suggested CASC2 served as a sponge of miR-31-5p in CAL-27/DDP and SCC9/DDP cells.

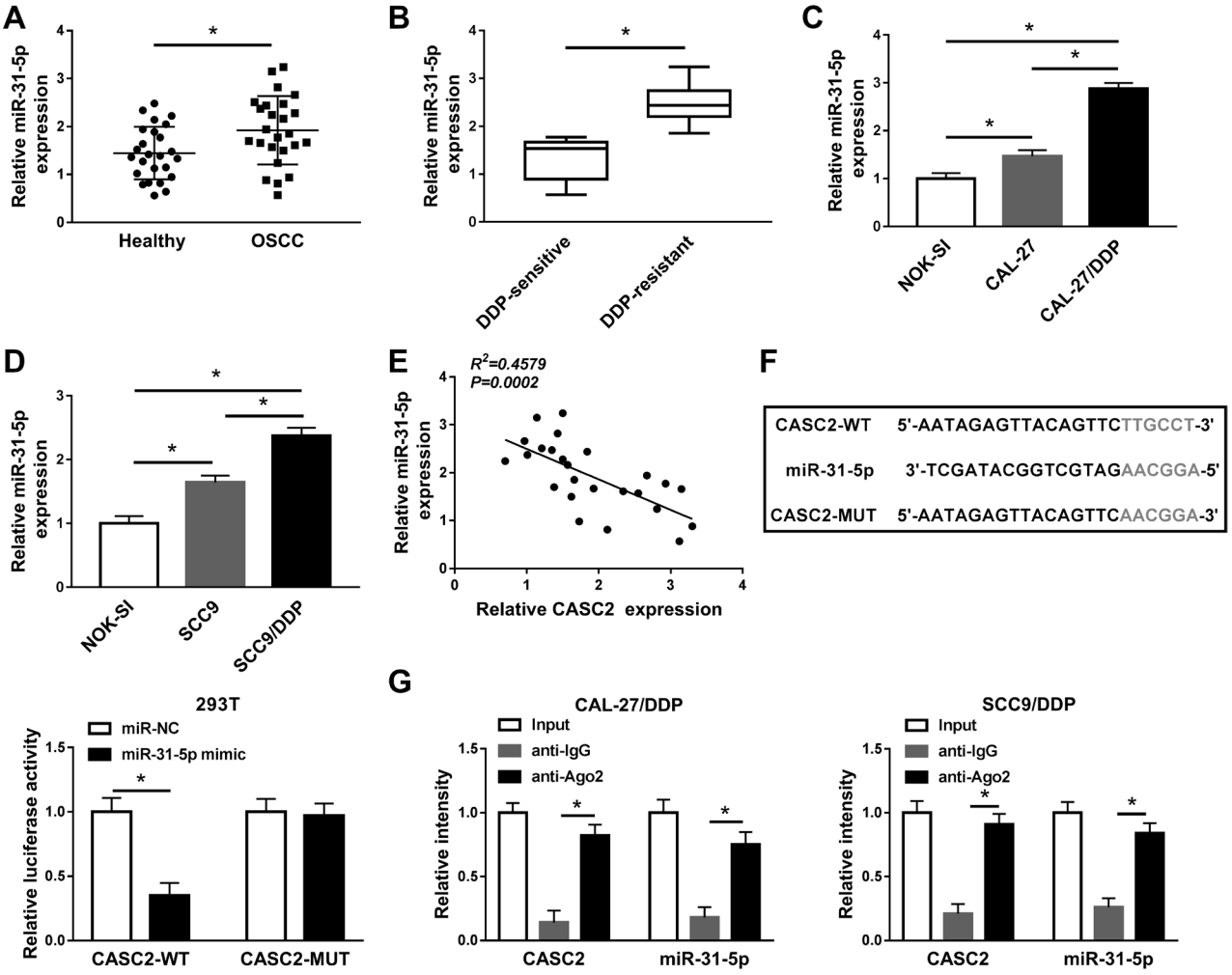

Figure 3. CASC2 was identified to serve as a sponge of miR-31-5p. A, B) qRT-PCR was utilized for the detection of the expression of miR-31-5p in 25 paired OSCC tissues and adjacent healthy tissues as well as 13 DDP-resistant OSCC tissues and 12 DDP-sensitive OSCC tissues. C, D) qRT-PCR was executed for the assessment of the expression of miR-31-5p in NOK-SI, CAL-27, SCC9, CAL-27/DDP, and SCC9/DDP cells. E) The correlation between miR-31-5p and CASC2 expression in OSCC tissues was analyzed by the Spearman's correlation analysis. F) The binding sites of CASC2 in miR-31-5p were predicted and verified via miRcode tool and dual-luciferase reporter assay. G) RIP assay was employed to verify the relationship between miR-31-5p and CASC2 in CAL-27/DDP and SCC9/DDP cells. Comparisons between two groups were executed by Student's *t* test, and comparisons among multiple groups were evaluated by ANOVA followed by Tukey post-hoc test. Data were exhibited as mean ± standard deviation. *p<0.05

miR-31-5p enhancement overturned CASC2 upregulation-mediated DDP sensitivity and cell apoptosis in DDP-resistant OSCC cells. Knowing that CASC2 acted as a sponge of miR-31-5p in CAL-27/DDP and SCC9/DDP cells, we further explored whether CASC2 exerted its role via miR-31-5p in DDP-resistant OSCC cells. We firstly transfected Vector, Over-CASC2, Over-CASC2+miR-NC, or Over-CASC2+miR-31-5p mimic into CAL-27/DDP and SCC9/DDP cells for the detection of the expression of miR-31-5p in CAL-27/DDP and SCC9/DDP cells. As shown in Figure 4A, the expression of miR-31-5p was significantly declined in AL-27/DDP and SCC9/DDP cells transfected with Over-CASC2, while this decrease was reversed by the introduction of miR-31-5p mimic. Afterward, the effects of miR-31-5p overexpression on DDP sensitivity and cell apoptosis in CASC2-elevated AL-27/DDP and SCC9/DDP cells were investigated. The CCK-8 assay manifested that both the inhibition of viability and the reduction of IC50 value of AL-27/DDP and SCC9/DDP cells induced by CASC2 overexpression were restored by miR-31-5p augmentation (Figures 4B, 4C). Also, flow cytometry assay revealed that augmented miR-31-5p expression abrogated the simulative effect of CASC2 introduction on the apoptosis of AL-27/DDP and SCC9/DDP cells (Figure 4D). Additionally, western blot analysis presented that overexpression of miR-31-5p abolished CASC2 increase-mediated the protein expression levels of Bax, Bcl-2, and MRP-1 in CAL-27/DDP and SCC9/DDP cells (Figure 4E). Taken together, these data indicated that CASC2 exerted its function by miR-31-5p in DDP-resistant OSCC cells.

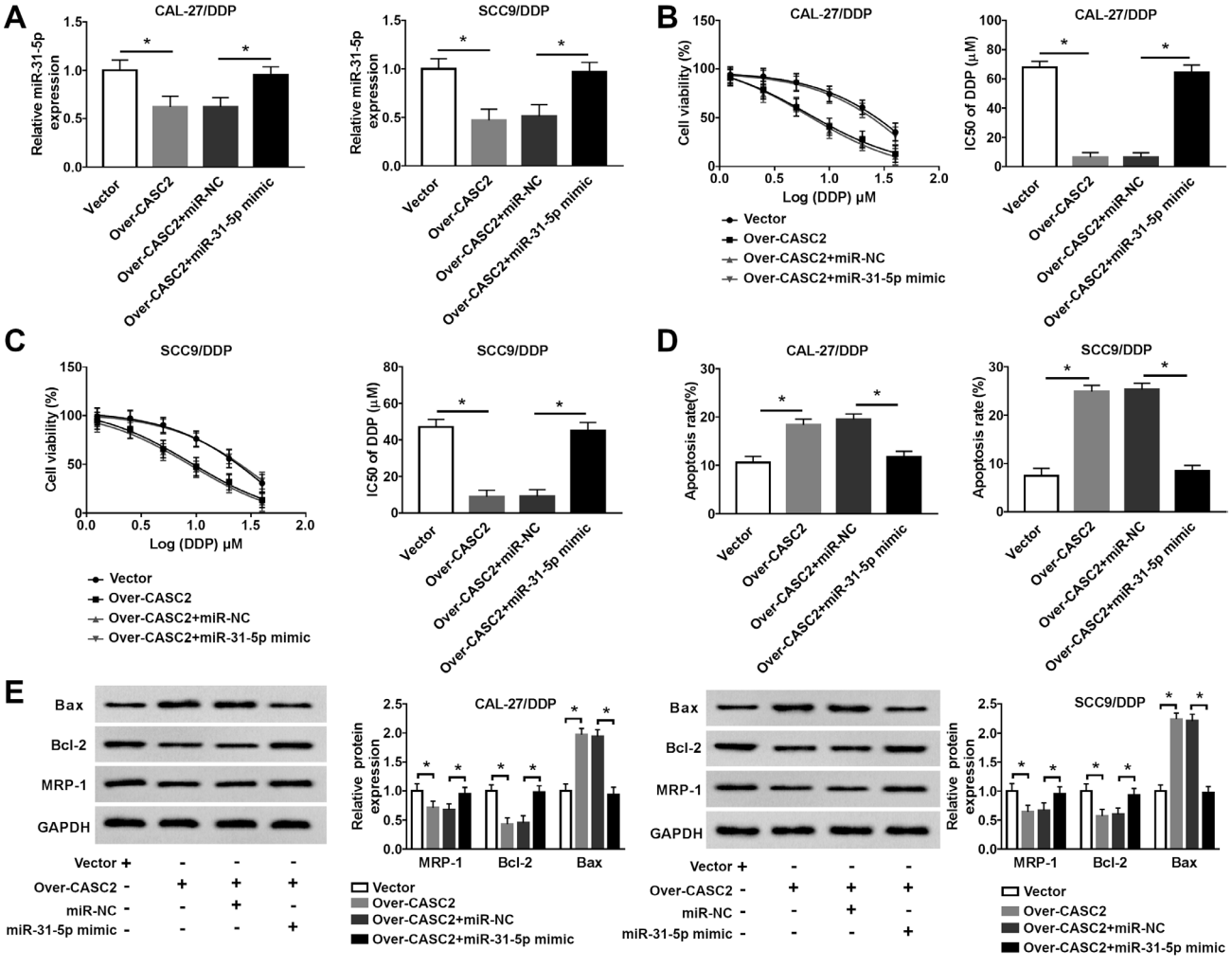

Figure 4. Effects of miR-31-5p elevation on CASC2 upregulation-mediated cell chemosensitivity in DDP-resistant OSCC cells. A–E) CAL-27/DDP and SCC9/DDP cells were transfected with Vector, Over-CASC2, Over-CASC2+miR-NC, or Over-CASC2+miR-31-5p mimic. (A) The expression of miR-31-5p in CAL-27/DDP and SCC9/DDP cells was detected with qRT-PCR. (B–C) The CCK-8 assay was utilized for analysis of the viability and IC50 value of CAL-27/DDP (B) and SCC9/DDP cells (C). (D) The apoptosis rate of CAL-27/DDP and SCC9/DDP cells was determined through flow cytometry assay. (E) The protein levels of Bax, Bcl-2, and MRP-1 in CAL-27/DDP and SCC9/DDP cells were probed via western blot analysis. Comparisons among multiple groups were evaluated by ANOVA followed by Tukey post-hoc test. Data were exhibited as mean ± standard deviation. *p<0.05

KANK1 acted as a target of miR-31-5p. Based on the above results, we further investigated the relationship between miR-31-5p and KANK1 in DDP-resistant OSCC cells. The results from qRT-PCR manifested that an apparent downregulation of KANK1 mRNA was seen in OSCC tissues compared to the adjacent healthy tissues (Figure 5A). Moreover, compared to the DDP-sensitive OSCC tissues, the expression of KANK1 mRNA was substantially decreased in DDP-resistant OSCC tissues (Figure 5B). Western blot analysis showed that the expression of KANK1 protein was effectively reduced in OSCC tissues than adjacent healthy tissues (Figure 5C). Uniformly, KANK1 mRNA and protein levels were exceptionally downregulated in CAL-27, SCC9, CAL-27/DDP, and SCC9/DDP cells than that in NOK-SI cells, and KANK1 mRNA and protein levels were strikingly lower in CAL-27/DDP and SCC9/DDP cells in comparison to the CAL-27 and SCC9 cells (Figures 5D, 5E). Also, the expression of KANK1 was negatively correlated with miR-31-5p in OSCC tissues (Figure 5F). Besides, we found that KANK1 contained the potential binding sites for miR-31-5p through the starBase 2.0 (Figure 5G). Then, we executed the dual-luciferase reporter assay to verify this prediction. The results exhibited that the luciferase activity of KANK1 3'UTR-WT was drastically attenuated in 293T cells transfected with miR-31-5p mimic, while the luciferase activity of KANK1 3'UTR-MUT did not vary (Figure 5G). Collectively, these results revealed that KANK1 served as a target of miR-31-5p in OSCC cells.

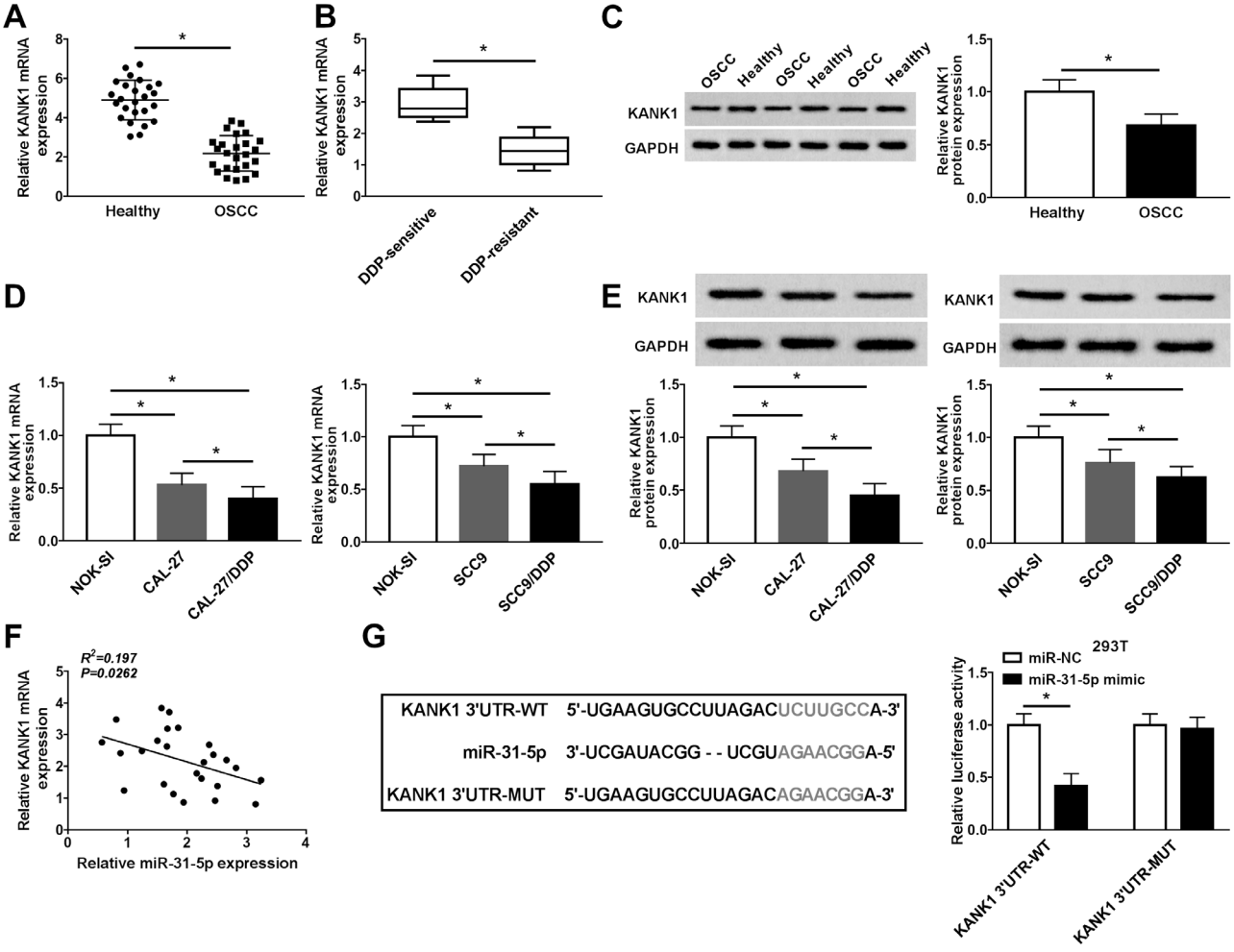

Figure 5. KANK1 served as a target of miR-31-5p. A, B) The expression of KANK1 mRNA in 25 paired OSCC tissues and adjacent healthy tissues (A), as well as 13 DDP-resistant OSCC tissues and 12 DDP-sensitive OSCC tissues (B), was measured via qRT-PCR. C) The expression of KANK1 protein in 25 paired OSCC tissues and adjacent healthy tissues was assessed with western blot analysis. D, E) qRT-PCR and western blot analysis were performed to analyze the expression of KANK1 mRNA (D) and protein (E) in NOK-SI, CAL-27, SCC9, CAL-27/DDP, and SCC9/DDP cells. F) Spearman's correlation analysis was applied to assess the correlation between KANK1 and miR-31-5p expression in OSCC tissues. G) The binding sites between miR-31-5p and KANK1 were predicted and verified via the starBase 2.0 database and dual-luciferase reporter assay. Comparisons between two groups were executed by Student's *t* test, and comparisons among multiple groups were evaluated by ANOVA followed by Tukey post-hoc test. Data were exhibited as mean ± standard deviation. *p<0.05

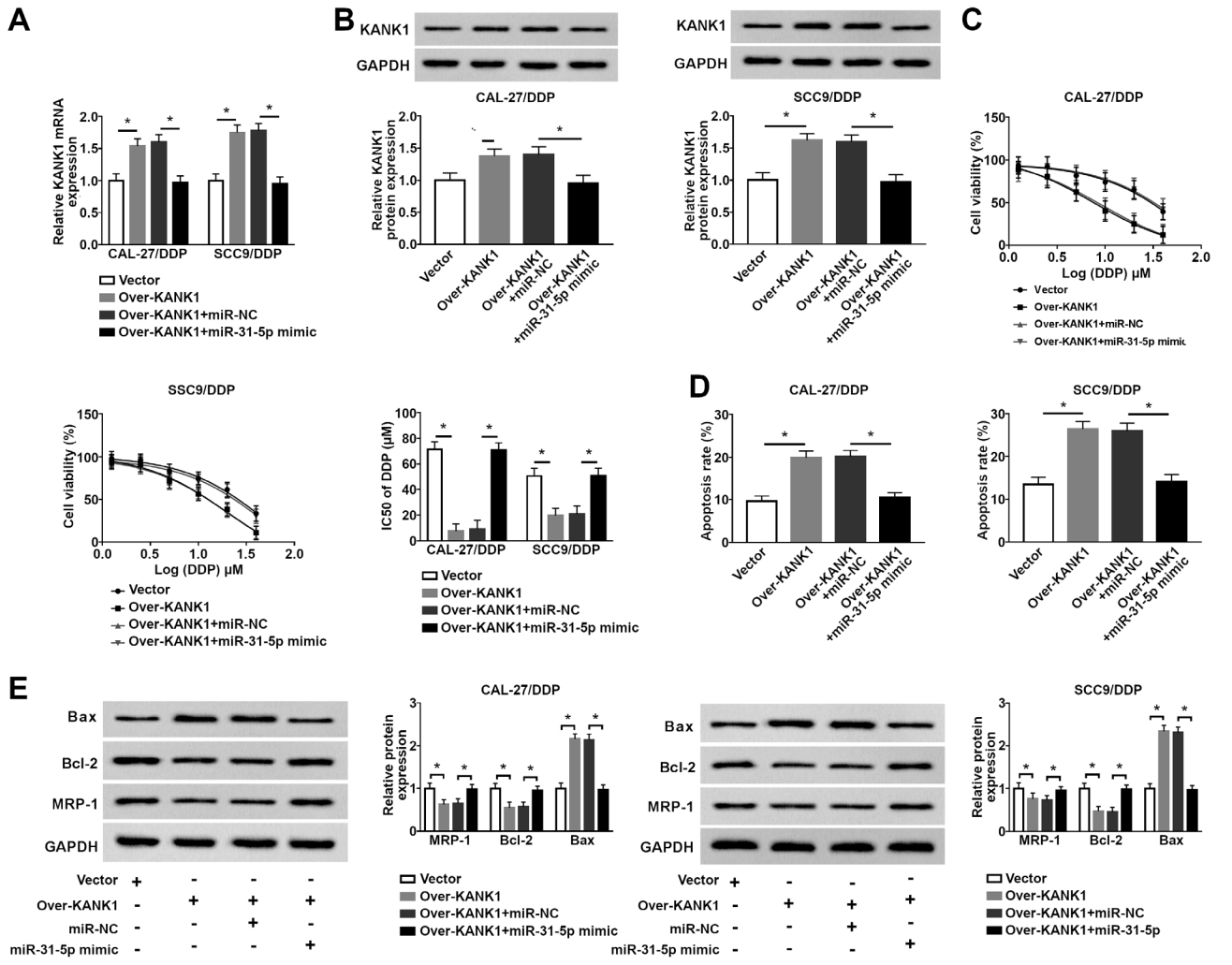

Figure 6. Effects of miR-31-5p enhancement on the KANK1 upregulation-mediated cell chemosensitivity in DDP-resistant OSCC cells. A–E) CAL-27/DDP and SCC9/DDP cells were transfected with Vector, Over-KANK1, Over-KANK1+miR-NC, or Over-KANK1+miR-31-5p mimic. The mRNA (A) and protein (B) levels of KANK1 in CAL-27/DDP and SCC9/DDP cells were detected with qRT-PCR or western blot analysis. (C) The CCK-8 assay was executed for the assessment of the viability and IC50 value of CAL-27/DDP and SCC9/DDP cells. (D) The apoptosis of CAL-27/DDP and SCC9/DDP cells was analyzed by flow cytometry assay. (E) Western blot analysis was used for the detection of the protein levels of Bax, Bcl-2, and MRP-1 in CAL-27/DDP and SCC9/DDP cells. Comparisons among multiple groups were evaluated by ANOVA followed by Tukey post-hoc test. Data were exhibited as mean ± standard deviation. *p<0.05

miR-31-5p upregulation reversed the effects of KANK1 upregulation on DDP sensitivity and cell apoptosis in DDP-resistant OSCC cells. It had been clarified that KANK1 served as a target of miR-31-5p in OSCC cells, and then we probed whether miR-31-5p played its role via KANK1 in DDP-resistant OSCC cells. qRT-PCR and western blot analysis manifested that the expression levels of KANK1 mRNA and protein were effectively enhanced in CAL-27/DDP and SCC9/DDP cells transfected with Over-KANK1, while these effects were reversed by the introduction of miR-31-5p mimic (Figures 6A, 6B). Next, we investigated the effects of miR-31-5p overexpression on KANK1 upregulation-mediated DDP sensitivity and cell apoptosis in CAL-27/DDP and SCC9/DDP cells. Results of the CCK-8 assay indicated that the miR-31-5p overexpression abolished both the constraint of viability and the decrease of IC50 value of CAL-27/DDP and SCC9/DDP cells caused by KANK1 augmentation (Figure 6C). Moreover, the elevation of the apoptosis rate of CAL-27/DDP and SCC9/DDP cells induced by KANK1 enhancement was recovered by miR-31-5p upregulation (Figure 6D). In addition, western blot analysis displayed that KANK1 upregulation caused both the increase of Bax protein and the downregulation of Bcl-2 and MRP-1 proteins, while these influences were reversed by the upregulation of miR-31-5p (Figure 6E). Overall, these findings suggested that miR-31-5p played its role via KANK1 in DDP-resistant OSCC cells.

CASC2 modulated KANK1 expression via sponging miR-31-5p. Then, we further quested whether CASC2 regulated the expression of KANK1 via miR-31-5p in CAL-27/DDP and SCC9/DDP cells. Results of qRT-PCR and western blot analysis demonstrated that the mRNA and protein levels of KANK1 in CAL-27/DDP and SCC9/DDP cells transfected with Over-CASC2 were especially upregulated, while this augmentation was reverted by the introduction of miR-31-5p mimic (Figures 7A, 7B). Therefore, these data demonstrated that KANK1 was modulated by CASC2 via sponging miR-31-5p in DDP-resistant OSCC cells.

CASC2 upregulation elevated DDP sensitivity and cell apoptosis in DDP-resistant OSCC cells *in vivo*. Considering that upregulation of CASC2 in DDP-resistant OSCC cells *in vitro* could elevate the chemosensitivity of DDP-resistant OSCC cells to DDP and promote cell apoptosis in DDP-resistant OSCC cells, we performed the mouse OSCC xenograft experiment to verify this conclusion *in vivo*. We constructed the SCC9/DDP cell line with a stable CASC2 overexpression (Over-CASC2) mediated by lentivirus and a control cell line (Vector), and injected them into mice and then treated with DDP. The results exhibited that compared with the control group with DDP treatment and CASC2 overexpression group without DDP treatment, the volume and weight of tumors were effectively impeded in the CASC2 enhancement group with DDP treatment (Figures 8A, 8B). Also, western blot analysis showed that Bax protein was upregulated while Bcl-2 and MRP-1 proteins were downregulated in the CASC2 elevation group with DDP treatment in contrast to the control group with DDP treatment and CASC2 augmentation group without DDP treatment (Figure 8C). Overall, these data suggested that CASC2 augmentation enhanced DDP sensitivity and induced cell apoptosis in DDP-resistant OSCC cells *in vivo*.

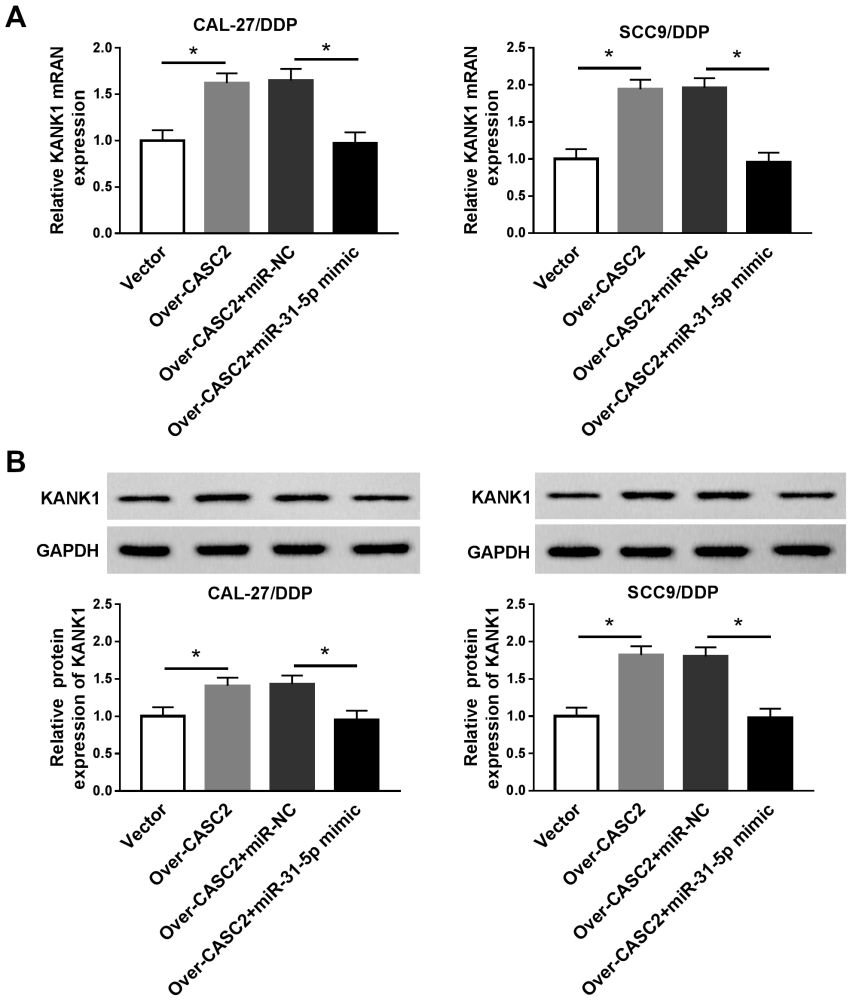

Figure 7. CASC2 modulated KANK1 expression via miR-31-5p. A, B) The mRNA (A) and protein (B) levels of KANK1 in CAL-27/DDP and SCC9/DDP cells transfected with Vector, Over-CASC2, Over-CASC2+miR-NC, or Over-CASC2+miR-31-5p mimic were analyzed by qRT-PCR or Western blot analysis. Comparisons among multiple groups were evaluated by ANOVA followed by Tukey post-hoc test. Data were exhibited as mean ± standard deviation. *p<0.05.

Discussion

OSCC accounts for about 3% and 90% of all clinical cancer cases and oral malignancies, respectively [42, 43]. LncRNAs have been reported to possess the hope as prospective new targets for the treatment of OSCC [44]. It had been pointed out that CASC2 curbed the progression of OSCC [16, 35]. Also, CASC2 was associated with the chemoresistance of multifarious tumors [13, 15, 45–46]. Li et al. disclosed that CASC2 introduction enhanced the sensitivity of temozolomide-resistant glioma cells to temozolomide [13]. Moreover, silenced CASC2 expression decreased the DDP sensitivity in gastric cancer and cervical cancer [43, 46]. Another study also revealed that upregulated CASC2 expression reduced the chemoresistance of prostate cancer cells to docetaxel [47]. The results of this study were consistent with the above studies, suggesting that high CASC2 expression enhanced the chemosensitivity of DDP-resistant OSCC cells to DDP. However, Zheng et al. claimed that CASC2 reduced paclitaxel chemosensitivity in breast cancer, which might be related to the tissue specificity of CASC2 [47].

Additionally, CASC2 was uncovered as a competing endogenous RNA of miR-21 in OSCC [16]. In the present study, we identified that miR-31-5p acted as a target of CASC2. miR-31-5p was claimed to boost the tumorigenicity of OSCC [23]. Moreover, miR-31-5p accelerated sorafenib resistance in renal cell cancer [21]. Likewise, miR-31-5p decreased the sensitivity of hepatocellular cancer cells to oxaliplatin [22]. In our study, miR-31-5p introduction reversed CASC2 upregulation-mediated DDP sensitivity and apoptosis in DDP-resistant OSCC cells. Therefore, we concluded that CASC2 mediated DDP sensitivity in DDP-resistant OSCC cells via miR-31-5p.

A series of studies had shown that KANK1 exerted an anticancer role in various tumors. For instance, increased KANK1 expression curbed the progression of gastric cancer [23] and lung cancer [28]. Moreover, KANK1 enhancement repressed cell cycle and accelerated cell apoptosis in brain glioma [48]. Fan et al. uncovered that KANK1 upregulation boosted cell apoptosis and suppressed cell proliferation in OSCC [49]. In our current research, KANK1 was regulated by CASC2 via miR-31-5p. Also, miR-31-5p augmenta-

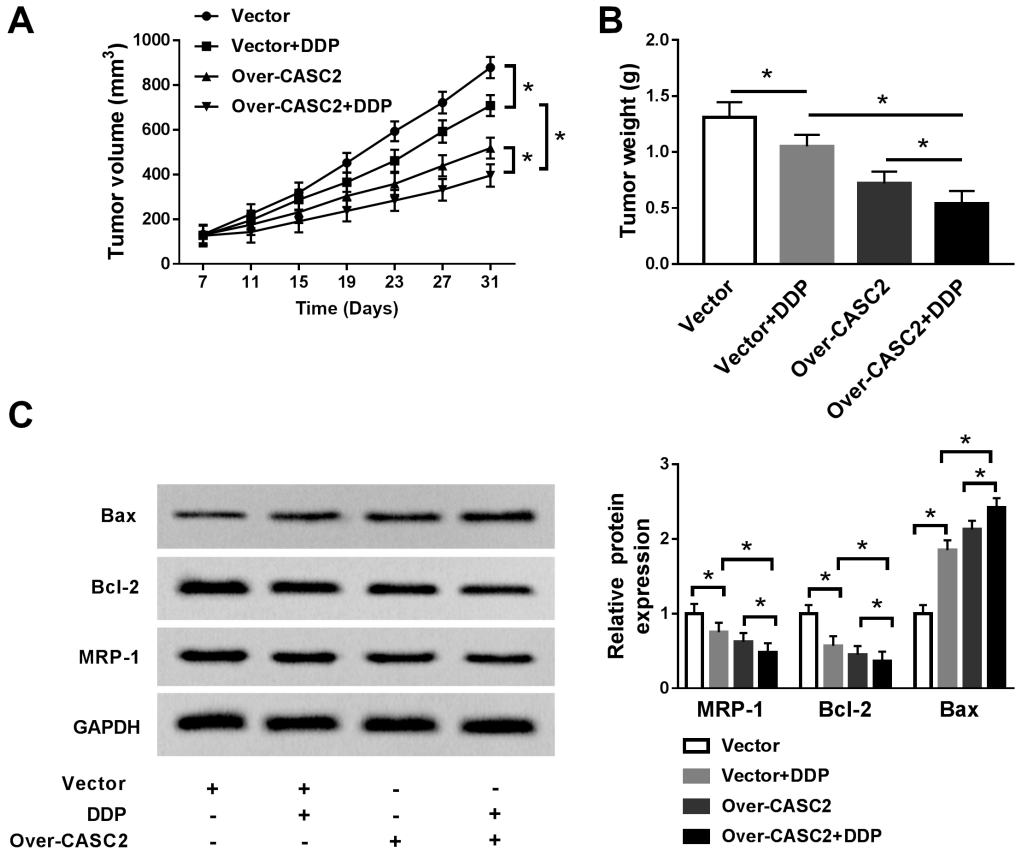

Figure 8. Effects of CASC2 upregulation on the chemosensitivity of DDP-resistant OSCC cells to DDP *in vivo*. A) Tumor volume curves for the Vector and Over-CASC2 groups with or without DDP treatment were measured every 4 days from day 7. B) Tumor weight was assessed for the Vector and Over-CASC2 groups with or without DDP treatment after day 31. C) The protein levels of Bax, Bcl-2, and MRP-1 in the Vector and Over-CASC2 groups with or without DDP treatment were assessed via western blot analysis. Comparisons among multiple groups were evaluated by ANOVA followed by Tukey post-hoc test. Data were exhibited as mean ± standard deviation. *p<0.05

tion restored the enhancement of DDP sensitivity and cell apoptosis in DDP-resistant OSCC cells caused by KANK1 overexpression. So, we inferred that KANK1-mediated DDP sensitivity in DDP-resistant OSCC cells through modulating KANK1 via miR-31-5p.

In sum, we concluded that CASC2 boosted the sensitivity of OSCC cells to DDP through upregulating KANK1 via miR-31-5p. This research provided a possible strategy for helping the therapy of DDP-resistant OSCC.

Acknowledgements: This study was supported by Qingdao Key Health Discipline Development Fund [No. 2020-2022].

References

[1] KIM SY, NAM SY, CHOI SH, CHO KJ, ROH JL. Prognostic value of lymph node density in node-positive patients with oral squamous cell carcinoma. Ann Surg Oncol 2011; 18: 2310–2317. https://doi.org/10.1245/s10434-011-1614-6

[2] PARIKH P, PATIL V, AGARWAL JP, CHATURVEDI P, VAIDYA A et al. Guidelines for treatment of recurrent or metastatic head and neck cancer. Indian J Cancer 2014; 51: 89–94. https://doi.org/10.4103/0019-509x.137896

[3] KESSLER P, GRABENBAUER G, LEHER A, BLOCH-BIRKHOLZ A, VAIRAKTARIS E et al. Neoadjuvant and adjuvant therapy in patients with oral squamous cell carcinoma Long-term survival in a prospective, non-randomized study. Br J Oral Maxillofac Surg 2008; 46: 1–5. https://doi.org/10.1016/j.bjoms.2007.08.006

[4] TANVETYANON T, PADHYA T, MCCAFFREY J, KISH JA, DECONTI RC et al. Postoperative concurrent chemotherapy and radiotherapy for high-risk cutaneous squamous cell carcinoma of the head and neck. Head Neck 2015; 37: 840–845. https://doi.org/10.1002/hed.23684

[5] KREPPEL M, DREISEIDLER T, ROTHAMEL D, EICH HT, DREBBER U et al. The role of clinical versus histopathological staging in patients with advanced oral squamous cell carcinoma treated with neoadjuvant radiochemotherapy followed by radical surgery. J Craniomaxillofac Surg 2013; 41: 22–27. https://doi.org/10.1016/j.jcms.2012.05.005

[6] MUNOZ GUERRA MF, NAVAL GIAS L, CAMPO FR, PEREZ JS. Marginal and segmental mandibulectomy in patients with oral cancer: a statistical analysis of 106 cases. J Oral Maxillofac Surg 2003; 61: 1289–1296. https://doi.org/10.1016/s0278-2391(03)00730-4

[7] FLOREA AM, BUSSELBERG D. Cisplatin as an anti-tumor drug: cellular mechanisms of activity, drug resistance and induced side effects. Cancers (Basel) 2011; 3: 1351–1371. https://doi.org/10.3390/cancers3011351

[8] ZHANG H, CHEN Z, WANG X, HUANG Z, HE Z et al. Long non-coding RNA: a new player in cancer. J Hematol Oncol 2013; 6: 37. https://doi.org/10.1186/1756-8722-6-37

[9] SCHMITZ SU, GROTE P, HERRMANN BG. Mechanisms of long noncoding RNA function in development and disease. Cell Mol Life Sci 2016; 73: 2491–2509. https://doi.org/10.1007/s00018-016-2174-5

[10] ABU N, HON KW, JEYARAMAN S, JAMAL R. Long non-coding RNAs as biotargets in cisplatin-based drug resistance. Future Oncol 2018; 14: 3085–3095. https://doi.org/10.2217/fon-2018-0303

[11] FANG Z, ZHAO J, XIE W, SUN Q, WANG H et al. LncRNA UCA1 promotes proliferation and cisplatin resistance of oral squamous cell carcinoma by sunppressing miR-184 expression. Cancer Med 2017; 6: 2897–2908. https://doi.org/10.1002/cam4.1253

[12] PALMIERI G, PALIOGIANNIS P, SINI MC, MANCA A, PALOMBA G et al. Long non-coding RNA CASC2 in human cancer. Crit Rev Oncol Hematol 2017; 111: 31–38. https://doi.org/10.1016/j.critrevonc.2017.01.003

[13] LIAO Y, SHEN L, ZHAO H, LIU Q, FU J et al. LncRNA CASC2 interacts with miR-181a to modulate glioma growth and resistance to TMZ through PTEN pathway. J Cell Biochem 2017; 118: 1889–1899. https://doi.org/10.1002/jcb.25910

[14] JIN X, CAI L, WANG C, DENG X, YI S et al. CASC2/miR-24/miR-221 modulates the TRAIL resistance of hepatocellular carcinoma cell through caspase-8/caspase-3. Cell Death Dis 2018; 9: 318. https://doi.org/10.1038/s41419-018-0350-2

[15] FENG Y, ZOU W, HU C, LI G, ZHOU S et al. Modulation of CASC2/miR-21/PTEN pathway sensitizes cervical cancer to cisplatin. Arch Biochem Biophys 2017; 623–624: 20–30. https://doi.org/10.1016/j.abb.2017.05.001

[16] PAN L, CHEN H, BAI Y, WANG Q, CHEN L. Long non-coding RNA CASC2 serves as a ceRNA of microRNA-21 to promote PDCD4 expression in oral squamous cell carcinoma. Onco Targets Ther 2019; 12: 3377–3385. https://doi.org/10.2147/ott.s198970

[17] MICHLEWSKI G, CACERES JF. Post-transcriptional control of miRNA biogenesis. RNA 2019; 25: 1–16. https://doi.org/10.1261/rna.068692.118

[18] KROL J, LOEDIGE I, FILIPOWICZ W. The widespread regulation of microRNA biogenesis, function and decay. Nat Rev Genet 2010; 11: 597–610. https://doi.org/10.1038/nrg2843

[19] PENG H, WANG L, SU Q, YI K, DU J et al. MiR-31-5p promotes the cell growth, migration and invasion of colorectal cancer cells by targeting NUMB. Biomed Pharmacother 2019; 109: 208–216. https://doi.org/10.1016/j.biopha.2018.10.048

[20] LI Y, QUAN J, CHEN F, PAN X, ZHUANG C et al. MiR-31-5p acts as a tumor suppressor in renal cell carcinoma by targeting cyclin-dependent kinase 1 (CDK1). Biomed Pharmacother 2019; 111: 517–526. https://doi.org/10.1016/j.biopha.2018.12.102

[21] HE J, HE J, MIN L, HE Y, GUAN H et al. Extracellular vesicles transmitted miR-31-5p promotes sorafenib resistance by targeting MLH1 in renal cell carcinoma. Int J Cancer 2019. https://doi.org/10.1002/ijc.32543

[22] QUE KT, ZHOU Y, YOU Y, ZHANG Z, ZHAO XP et al. MicroRNA-31-5p regulates chemosensitivity by preventing the nuclear location of PARP1 in hepatocellular carcinoma. J Exp Clin Cancer Res 2018; 37: 268. https://doi.org/10.1186/s13046-018-0930-0

[23] LAI YH, LIU H, CHIANG WF, CHEN TW, CHU LJ et al. MiR-31-5p-ACOX1 axis enhances tumorigenic fitness in oral squamous cell carcinoma via the promigratory prostaglandin E2. Theranostics 2018; 8: 486–504. https://doi.org/10.7150/thno.22059

[24] GAO Z, WANG H, LI H, LI M, WANG J et al. Long non-coding RNA CASC2 inhibits breast cancer cell growth and metastasis through the regulation of the miR-96-5p/SYVN1 pathway. Int J Oncol 2018; 53: 2081–2090. https://doi.org/10.3892/ijo.2018.4522

[25] CHEN NP, SUN Z, FÄSSLER R. The Kank family proteins in adhesion dynamics. Curr Opin Cell Biol 2018; 54: 130–136. https://doi.org/10.1016/j.ceb.2018.05.015

[26] BOUCHET BP, GOUGH RE, AMMON YC, VAN DE WILLIGE D, POST H et al. Talin-KANK1 interaction controls the recruitment of cortical microtubule stabilizing complexes to focal adhesions. Elife 2016; 5: e18124. https://doi.org/10.7554/eLife.18124

[27] SUZUKI JI, ROY BC, OGAERI T, KAKINUMA N, KIYAMA R. Depletion of tumor suppressor Kank1 induces centrosomal amplification via hyperactivation of RhoA. Exp Cell Res 2017; 353: 79–87. https://doi.org/10.1016/j.yexcr.2017.03.006

[28] GU Y, ZHANG M. Upregulation of the Kank1 gene inhibits human lung cancer progression in vitro and in vivo. Oncol Rep 2018; 40: 1243–1250. https://doi.org/10.3892/or.2018.6526

[29] CUI Z, SHEN Y, CHEN KH, MITTAL SK, YANG JY et al. KANK1 inhibits cell growth by inducing apoptosis through regulating CXXC5 in human malignant peripheral nerve sheath tumors. Sci Rep 2017; 7: 40325. https://doi.org/10.1038/srep40325

[30] BARNES L, EVESON JW, REICHART P, SIDRANSKY S. (Eds.). World Health Organization Classification of Tumours. Pathology and Genetics of Head and Neck Tumours. IARC Press, Lyon 2005, p 435. ISBN 92 832 2417 5

[31] CHEN T, WANG K, TONG X. In vivo and in vitro inhibition of human gastric cancer progress by upregulating Kank1 gene. Oncol Rep 2017; 38: 1663–1669. https://doi.org/10.3892/or.2017.5823

[32] LANIOSZ V, TORGERSON RR, RAMOS-RODRIGUEZ AJ, MA JE, MARA KC et al., Incidence of squamous cell carcinoma in oral lichen planus: a 25-year population-based study. Int J Dermatol 2019; 58: 296–301. https://doi.org/10.1111/ijd.14215

[33] MATTHIAS T, SELGAI H, SOPHIE B, MARKUS T, PROBST FA et al. What factors are associated with regional recurrence following operative treatment of oral squamous cell carcinoma? Int J Dermatol 2019; 58: 296–301. https://doi.org/10.1111/ijd.14215

[34] GOSEPATH EM, ECKSTEIN N, HAMACHER A, SERVAN K, VON JONQUIERES G et al. Acquired cisplatin resistance in the head-neck cancer cell line Cal27 is associated with decreased DKK1 expression and can partially be reversed by overexpression of DKK1. Int J Cancer 2008; 123: 2013–2019. https://doi.org/10.1002/ijc.23721

[35] YAN P, SU Z, ZHANG Z, GAO T. LncRNA NEAT1 enhances the resistance of anaplastic thyroid carcinoma cells to cisplatin by sponging miR95p and regulating SPAG9 expression. Int J Oncol 2019; 55: 988–1002. https://doi.org/10.3892/ijo.2019.4868

[36] LIVAK KJ, SCHMITTGEN TD. Analysis of relative gene expression data using real-time quantitative PCR and the 2(-Delta Delta C(T)) Method. Methods 2001; 25: 402–408. https://doi.org/10.1006/meth.2001.1262

[37] XING HB, QIU HM, LI Y, DONG PF, ZHU XM. Long non-coding RNA CASC2 alleviates the growth, migration and invasion of oral squamous cell carcinoma via downregulating CDK1. Eur Rev Med Pharmacol Sci 2019; 23: 4777–4783. https://doi.org/10.26355/eurrev_201906_18060

[38] YANG DW, QIAN GB, JIANG MJ, WANG P, WANG KZ. Inhibition of microRNA-495 suppresses chondrocyte apoptosis through activation of the NF-κB signaling pathway by regulating CCL4 in osteoarthritis. Gene Ther 2019; 26: 217–229. https://doi.org/10.1038/s41434-019-0068-5

[39] MISHRA R, NAGINI S, RANA A. Expression and inactivation of glycogen synthase kinase 3 alpha/ beta and their association with the expression of cyclin D1 and p53 in oral squamous cell carcinoma progression. Mol Cancer 2015; 14: 20. https://doi.org/10.1186/s12943-015-0300-x

[40] WANG Y, LIU Z, YAO B, DOU C, XU M et al. Long non-coding RNA TUSC7 acts a molecular sponge for miR-10a and suppresses EMT in hepatocellular carcinoma. Tumour Biol 2016; 37: 11429–11441. https://doi.org/10.1007/s13277-016-4892-6

[41] ZHANG Y, LIU Y, XU X. Knockdown of LncRNA-UCA1 suppresses chemoresistance of pediatric AML by inhibiting glycolysis through the microRNA-125a/hexokinase 2 pathway. J Cell Biochem 2018; 119: 6296–6308. https://doi.org/10.1002/jcb.26899

[42] FANG Z, ZHAO J, XIE W, SUN Q, WANG H et al. LncRNA UCA1 promotes proliferation and cisplatin resistance of oral squamous cell carcinoma by sunppressing miR-184 expression. Cancer Med 2017; 6: 2897–2908. https://doi.org/10.1002/cam4.1253

[43] KADEMANI D. Oral cancer. Mayo Clin Proc 2007; 82: 878–887. https://doi.org/10.4065/82.7.878

[44] ZHANG L, MENG X, ZHU XW, YANG DC, CHEN R et al. Long non-coding RNAs in Oral squamous cell carcinoma: biologic function, mechanisms and clinical implications. Mol Cancer 2019; 18: 102. https://doi.org/10.1186/s12943-019-1021-3

[45] GAO W, LIN S, CHENG C, ZHU A, HU Y et al. Long non-coding RNA CASC2 regulates Sprouty2 via functioning as a competing endogenous RNA for miR-183 to modulate the sensitivity of prostate cancer cells to docetaxel. Arch Biochem Biophys 2019; 665: 69–78. https://doi.org/10.1016/j.abb.2018.01.013

[46] LI Y, LV S, NING H, LI K, ZHOU X et al. Down-regulation of CASC2 contributes to cisplatin resistance in gastric cancer by sponging miR-19a. Biomed Pharmacother 2018; 108: 1775–1782. https://doi.org/10.1016/j.biopha.2018.09.181

[47] ZHENG P, DONG L, ZHANG B, DAI J, ZHANG Y et al. Long noncoding RNA CASC2 promotes paclitaxel resistance in breast cancer through regulation of miR-18a-5p/CDK19. Histochem Cell Biol 2019; 152: 281–291. https://doi.org/10.1007/s00418-019-01794-4

[48] GUO X, FAN W, BIAN X, MA D. Upregulation of the Kank1 gene-induced brain glioma apoptosis and blockade of the cell cycle in G0/G1 phase. Int J Oncol 2014; 44: 797–804. https://doi.org/10.3892/ijo.2014.2247

[49] FAN H, TIAN H, CHENG X, CHEN Y, LIANG S et al. Aberrant Kank1 expression regulates YAP to promote apoptosis and inhibit proliferation in OSCC. J Cell Physiol 2020; 235: 1850–1865. https://doi.org/10.1002/jcp.29102